Conical petal epidermal cells, regulated by the MYB transcription factor MIXTA, have an ancient origin within the angiosperms

Alison Reed[1], Paula J. Rudall[2], Samuel F. Brockington[1] and Beverley J. Glover[1*]

[1] Department of Plant Sciences, University of Cambridge, Downing Street, Cambridge, CB2 3EA, UK

[2] Jodrell Laboratory, Royal Botanic Gardens Kew, Richmond, Surrey, TW9 3AB, UK

[*] Correspondence: bjg26@cam.ac.uk

Running title: Conical petal epidermal cells

Submitted: 17 February 2022

Figures: 5, tables: 2.

Words: 5086

Highlight

We show that some of the earliest diverging flowers have pollinator-attracting conical cells, and provide evidence to suggest that the genetic pathway controlling their development is also ancient.

Abstract

Conical epidermal cells occur on the tepals (perianth organs, typically petals and/or sepals) of the majority of animal-pollinated angiosperms, where they play both visual and tactile roles in pollinator attraction, providing grip to foraging insects and enhancing colour, temperature and hydrophobicity. To explore the evolutionary history of conical epidermal cells in angiosperms, we surveyed the tepal epidermis in representative species of the ANA-grade families, the early-diverging successive sister lineages to all other extant angiosperms, and analysed the function of a candidate regulator of cell outgrowth from *Cabomba caroliniana* (Nymphaeales). We identified conical cells in at least two genera from different families (*Austrobaileya*, *Cabomba*). A single *SBG9 MYB* gene was isolated from *C. caroliniana* and found to induce strong differentiation of cellular outgrowth, including conical cells, when ectopically expressed in *Nicotiana tabacum*. Ontogenetic analysis and quantitative RT-PCR established that *CcSBG9A1* is spatially and temporally expressed in a profile which correlates with a role in conical cell development. We conclude that conical or subconical cells on perianth organs are ancient within the angiosperms and most likely develop using a common genetic programme initiated by a SBG9 MYB transcription factor.

Keywords: ANA grade, *Cabomba caroliniana*, conical cell, MIXTA, Nymphaeales, papillae, petal, tepal

Introduction

The relationships between flowering plants and their pollinators are key components of ecological networks in almost all terrestrial habitats. Animal pollinators are diverse, with more than 20,000 pollinating bee species and numerous other insect and vertebrate pollinators (Kevan, 1999). An estimated 35 per cent of global crop production (by volume) depends on biotic pollination, and a decrease in pollinator numbers worldwide has led to a reduction in some crop production rates (Klein *et al*., 2007). The evolutionary radiation of angiosperms and their insect pollinators has resulted in considerable diversity of floral forms, with a range of floral traits thought to have evolved in response to selective pressure to increase floral attractiveness and memorability (Kevan and Baker, 1983; Schiestl and Johnson, 2013). These traits include flower scent and reward, as well as visual cues involving colour, shape and patterning.

In the majority of biotically-pollinated angiosperm species, the perianth organs involved in visual advertising to pollinators (the tepals or petals) have conical or papillate epidermal cells, at least on the adaxial surface (Kay *et al*., 1981, Christensen and Hansen, 1998, Ojeda *et al.*, 2009). The observation that conical cells are widespread on petals but rare on leaves indicates that they function to increase floral attractiveness and plant reproductive success, a hypothesis that is supported by field trials in which wild-type flowers of *Antirrhinum majus* with conical cells received more insect attention and set more fruit than otherwise isogenic *mixta* mutant flowers with flat cells (Glover and Martin, 1998). Conical cell shape not only focuses light into petals, enhancing the pigmented colour (Kay *et al*., 1981; Gorton and Vogelman, 1996; Dyer *et al*., 2007), but also provides a tactile advantage; bees can recognise different epidermal surfaces based on touch alone (Kevan and Lane, 1985; Whitney *et al*., 2009). Conical cells enable insects to minimise energy expenditure by ceasing wing movement and coming to rest while they feed, especially in natural conditions, when flowers are rarely stationary (Rands *et al*., 2011; Alcorn *et al*. (2012).

Conical tepal epidermal cells have been described across a phylogenetically broad range of angiosperm species, including many orders of eudicots and monocots (Kay *et al*., 1981, Christensen and Hansen, 1998, Ojeda *et al.*, 2009; Taneda *et al*., 2015). In contrast, relatively little is known about their distribution among the ANA-grade lineages (Amborellales, Nymphaeales, Austrobaileyales), which represent separate successive sister lineages to all other extant angiosperms in recent phylogenetic analyses (Fig. 1) (Angiosperm Phylogeny Group [APG] III, 2009). The seminal investigation of Kay *et al*. (1981) did not

include any ANA-grade families. Despite many morphological studies of flowers of ANA-grade species (e.g. Endress, 2008, 2010), existing descriptions of tepal surfaces are rare, with a few notable exceptions in the waterlily families Nymphaeaceae (Warner *et al*., 2008, 2009; Zini *et al*., 2017; Coiro and Barone Lumaga, 2018) and Cabombaceae (Vialette-Guiraud *et al*., 2011). To address these gaps, we explore the distribution of tepal epidermal cell morphologies across the ANA-grade orders.

The high morphological diversity among the relatively species-poor ANA-grade lineages, coupled with the absence of a closely related extant outgroup to angiosperms, make it difficult to reconstruct hypothetical ancestral states. However, extending information on both comparative morphology and gene function to the ANA-grade lineages is essential in understanding early angiosperm evolution. To explore these aspects, we analysed *MIXTA*-like gene function from an ANA-grade species that possesses conical cells: *Cabomba caroliniana* (Nymphaeales). In *Antirrhinum majus*, loss of activity of the *MIXTA* gene leads to loss of the conical cell phenotype (Noda *et al*., 1994), while ectopic expression of *MIXTA* in *Nicotiana tabacum* is sufficient to promote conical cell outgrowth (Glover *et al*., 1998). *MIXTA* is a member of the R2R3 MYB transcription factor family, a subset of the MYB-transcription-factor family that is unique to plants (Martin and Paz-Ares, 1997; Dubos *et al*., 2010). The R2R3 MYB transcription factors comprise 22 subgroups (Stracke *et al*., 2001), with *MIXTA* falling into subgroup 9 (SBG9). Since the identification of *AmMIXTA*, three other *SBG9* genes have been identified in *A. majus*: *MYB MIXTA*-like (*AmMYBML*) *1*, *2* and *3*, with overlapping but non-redundant functions (Perez-Rodriguez *et al*., 2005; Baumann *et al*., 2007; Jaffé *et al*., 2007).

Phylogenetic analysis of SBG9 R2R3 *MYB* genes has revealed an ancient duplication that occurred before the origin of seed plants, resulting in two strongly supported clades: Subgroup 9A (SBG9A, which encompasses *AmMIXTA* and *AmMYBML1*, *2* and *3*) and Subgroup 9B (Brockington *et al*., 2012). SBG9A *MYB* genes have now been functionally characterised from the basal eudicot *Thalictrum thalictroides* (Di Stilio *et al*., 2009), the monocot *Dendrobium crumenatum* (Gilding and Marks, 2010), and a range of eudicot species (Baumann *et al*., 2007; Machado *et al*., 2009; Gilding and Marks, 2010; Brockington *et al*., 2013). To date, the only SBG9B gene that has been characterised is *MYB17-like* from *Lotus japonicus* (Brockington *et al*., 2012). All SBG9 MYB transcription factors analysed so far play a role in epidermal cell outgrowth, often associated with petal conical cells.

The morphological data that we present here, exploring conical tepal epidermal cell distribution across the ANA grade angiosperms, combined with our analysis of SBG9 MYB

function in *Cabomba caroliniana*, suggests that conical petal epidermal cells, and the anisotropic cell expansion that underpins their development in eudicots, are an ancestral feature of flowering plants.

Materials and Methods

Sources of plant material

Material of ANA-grade angiosperms examined for morphology is indicated in Table 1. All *Cabomba caroliniana* flowers and vegetative tissues for RNA/DNA extraction were purchased online from Plants Alive Ltd (Stone, Staffordshire, UK) and grown in a glass aquarium in 10 × 3.5 cm round pots with rockwool, weighted down using lead strips.

Material preparation and preservation

Flowers and inflorescences were harvested and immediately fixed in FAA (60% ethanol; 6% formaldehyde; 5% acetic acid). The flowers were left in fixative for 72 hours and then transferred to 70% ethanol (EtOH) solution. Where fresh material was impractical to collect, dental wax (Elite HD vinylpolysiloxane) was used to make a high resolution mould of plant surfaces and accurate replicas were produced using Devcon 2 Ton epoxy resin.

Scanning electron microscopy

Prior to examination using Scanning Electron Microscopy (SEM), fixed samples (stored in 70% EtOH) were dehydrated in a series of ascending EtOH concentrations and critical point dried in an Autosamdri 815B critical point drier. Samples were sputter-coated in platinum using an Emitech K550 sputter coater. The coated specimens were viewed using a Hitachi FE-SEM S-4700 scanning electron microscope (Hitachi Hi-Tec Technologies, Maidenhead, UK) and images captured using PCI software (Quartz Imaging Corp., Vancouver, Canada). Epoxy cast material was coated in gold or chromium using a Quorum K756X sputter coater. Samples were then viewed using a FEI Philips XL30 FEGSEM Scanning electron microscope 0.5 - 30 KeV with Oxford Instruments INCA EDX system running a 30 mm^2 SiLi thin window pentafet EDX detector.

Isolation of CcSBG9A1

RNA was extracted from floral tissue frozen in liquid nitrogen, using a CTAB-based

extraction followed by chloroform extraction and precipitation in 4M LiCl. Prior to cDNA synthesis, RNA samples were treated with DNAse I. cDNA was synthesised from total RNA using Bioline Bioscript™ Reverse Transcriptase, and Oligo dT priming.
SBG9 R2R3 *MYB*-like sequences from ANA-grade angiosperms (*Amborella trichopoda* and *Nuphar* sp.) were obtained from the genomics database of the National Center for Biotechnology Information (NCBI; http://www.ncbi.nlm.nih.gov/). Sequences were aligned using Se-Al v2.0a11 and used to design degenerate primers. RACE was used to amplify full length cDNAs which were cloned into pGEM-T for sequencing and further analysis. Primer sequences are listed in Table S1.

Phylogenetic analysis

The putative *Cabomba* SBG9A protein was analysed in the context of previous published alignments generated for the SBG9A clade (Brockington et al., 2013). The sequence was aligned using the translation align function of nucleotide sequences in Geneious, and subject to a FastTree algorithm, using the GTR model. SH support values were generated during the FastTree analysis, and reported on the tree topology. All branches with less than 0.50 SH support were removed.

Ectopic expression in Nicotiana tabacum

The binary vector pGREENII0029:35S with the LacZ gene removed and replaced with a double copy of the cauliflower mosaic virus (CaMV) 35S gene promoter (Hellens *et al*., 2000) was used for gene transfer. *CcSBG9A-1* was inserted as an EcoRI fragment from pGEM-T into pGREEN. The binary vector was transferred into *Agrobacterium tumefaciens* GV3101 by electroporation. Transformation of *Nicotiana tabacum* var. Samsun was conducted using a modified version of the leaf disk protocol of Horsch *et al*. (1985). Transgenic plants were grown to maturity in a controlled greenhouse environment at 26^{o}C with a 16 hour light regime, and transgene insertion and expression confirmed using PCR with genomic DNA and RT-PCR with leaf RNA (Figure S1).

Quantitative RT-PCR (qPCR)

Mature flowers and buds were dissected on three independent plants using micro-dissecting forceps. Carpels, stamens and tepals were removed separately and immediately frozen in

liquid nitrogen. Forceps were cleaned with 100% ethanol between each tissue and flower. RNA for qPCR was extracted using Plant RNA Reagent (Invitrogen™), treated with Ambion TURBO DNA-free™ and converted to cDNA using Invitrogen Superscript III, primed using oligo(dT)20 and random hexamer. *CcActin* was selected as a reference gene based on successful preliminary trials demonstrating stable expression across tissues. Primer sequences are provided in Table S1. 40 cycles of PCR were performed using either a BioRad DNA Engine Thermocycler or a CFX Connect Real-Time PCR Detections System (185-5200). A melting curve was performed from 60ºC to 95ºC with readings taken at 0.5ºC intervals. Relative gene expression was quantified using Opticon Monitor 3 and CFX Manager software (both BioRad Laboratories, Inc). Ct values were exported to Microsoft Excel and ΔCt values calculated by subtracting the Ct of the reference gene, actin. Each data set was statistically analysed in Excel using a *t*-test.

Results

Conical or subconical tepal epidermal cells occur in several ANA-grade species

A summary of tepal surfaces of ANA-grade species is given in Table 2 and Fig. 2, with emphasis on the distribution of conical cells and surface patterning. Following the terminology outlined by Kay *et al*. (1981), conical cells and papillate cells are more or less synonymous; they protrude significantly outwards from the epidermis and have a distinct tip or peak (subconical cells slightly less so). Lenticular cells are only slightly domed and lack a distinct tip. Flat cells show no clear sign of protrusion. In surface view, cell shape ranges from rounded to elongated, often on the same petal, with elongated cells mostly occurring at the petal/tepal base. In transverse section, cell shape ranges from flat through domed/lenticular to conical – as noted above, the presence of a distinct tip or peak separates conical cells from domed cells. Fine details of surface sculpturing range from smooth to striate.

ANA-grade taxa display diverse tepal surface structure, consistent with their diverse floral morphology. Of the seven ANA-grade families, distinctly conical epidermal cells are present in species of *Austrobaileya* (Austrobaileyaceae), *Cabomba* (Cabombaceae) and the staminoid tepals of *Victoria cruziana* (Nymphaeaceae). In *Austrobaileya scandens*, conical cells cover most parts of the flower (tepals, stamens, staminodia) except the carpels and the central regions of the outer tepals; all cells and papillae possess fine radiating striations. The

adaxial tepal surface of *A. scandens* is complex, with large stomata and secretory cells also present; stomata are more abundant in central flat-celled regions that lack conical papillae. In *Cabomba*, non-striated conical cells cover the adaxial tepal surfaces of anthetic flowers, especially towards the tepal apex, with relatively flat surfaces at the tepal bases. In *Victoria cruziana*, only the innermost tepals and staminoid tepals have conical cells, which are often striated.

Subconical or deeply domed cells are present in *Amborella* (Amborellaceae), *Illicium* (Illiciaceae) and *Kadsura* (Schisandraceae). In *Amborella trichopoda*, the tepals are thick and reflexed, with a central adaxial groove surrounded by bulbous regions. The adaxial tepal surfaces display diverse morphology, though epidermal cells are mostly deeply domed, often flat-topped or angular with chaotic fine surface patterning. In *Illicium simmonsii*, tepal surfaces range from flat-celled to domed, sometimes with a central prominence and always with striations. In *Kadsura heteroclita*, most of the tepal surface is covered by subconical or occasionally conical cells. Conical and subconical cells are absent from Hydatellaceae, most Nymphaeaceae, *Schisandra* (Schisandraceae) and Trimeniaceae

Regulation of conical epidermal cell growth in Cabomba caroliniana

S*equence and phylogenetic placement of* CcSBG9A1 – To determine whether the anisotropic outgrowth of conical cells of ANA-grade tepals is regulated by the same R2R3MYB transcription factors (subgroup 9 MIXTA-like proteins) that control conical petal cell development in angiosperms, we isolated a SBG9A R2R3 *MYB* gene from *Cabomba caroliniana* using degenerate PCR. The predicted protein contains the amino acid motif that is characteristic of the SBG9A lineage, which contains the well-characterised *MIXTA* and *MIXTA-LIKE* genes from eudicots (Brockington *et al.*, 2013). The CcSBG9A1 protein shows a high degree of similarity with SBG9A MYB proteins from other ANA-grade genera. One notable exception is the occurrence of an amino acid substitution (lysine in place of threonine) at the centre of the highly conserved SBG9A motif. Phylogenetic analysis of SBG9A MYB genes, with the inclusion of the *CcSBG9A1* gene isolated here, confirms that *CcSBG9A1* groups with SBG9A MYB genes from other ANA-grade genera (*Nuphar* and *Amborella*) (Fig. 3, Supplementary Data Fig. S2). Together with monocot sequences and early diverging eudicot sequences, these ANA-grade sequences diverged before the main duplication within the core eudicots that gave rise to the *MIXTA* and *MIXTA*-like clades (Brockington *et al.*, 2013). While there are recent, lineage-specific duplications of this gene

family within *Amborella trichopoda* and *Nuphar advena*, there is no evidence from this analysis of a deep duplication event within the ANA-grade. Since our degenerate PCR identified no other gene fragments, there is only a single SBG9A EST from *Cabomba aquatica*, and our phylogenetic analysis provides no evidence of a deep duplication event, we tentatively conclude that there is only a single representative of MYB SBG9A in the *Cabomba* genome.

Transgenic analysis of CcSBG9A1 *function in a tobacco bioassay* – To explore the ability of the CcSBG9A1 protein to induce anisotropic cell expansion and cellular outgrowth, we generated nine independent transgenic lines of tobacco (*Nicotiana tabacum* var. Samsun) expressing the gene from the double CaMV35S promoter (Supplementary Data Figure S1). The same bioassay has been used to explore the function of eudicot members of this gene family with different genes able to induce cellular outgrowth on different subsets of tobacco organs (Glover *et al.*, 1998; Perez-Rodriguez *et al.*, 2005; Baumann *et al.*, 2007; Jaffe *et al.*, 2007; Brockington *et al.*, 2013). The transgenic plants displayed a reduction in flower colour, the transgenic flowers appearing a much paler shade of pink relative to wild-type lines (Fig. 4a). The anthers of several of these lines – those also showing the strongest change in epidermal phenotype – failed to fully dehisce. These phenotypic outcomes have been described in other studies expressing SBG9A *MYB* genes in tobacco (Glover *et al.*, 1998).

Previous studies have reported that the ectopic expression of SBG9A *MYB* genes in tobacco most commonly induces cell outgrowth on the ovary epidermis. In wild-type plants, epidermal cells of the ovary have a rounded base shape and are flat or slightly lenticular (Fig. 4b). In all lines of transgenic tobacco expressing 35S:*CcSBG9A1* ectopic cell outgrowths were present on the surface of the ovary (Fig. 4c). The majority of epidermal cells had an altered appearance and conical cells and trichomes were present in approximately equal abundance. These cell protrusions ranged from 10–350 μm in length.

In wild-type tobacco flowers, the style and stamen filaments have uniformly flat elongate cells (Fig. 4d). In transgenic lines expressing 35S:*CcSBG9A1*, ectopic cell protrusions were observed on both floral organs, although they were less dense than on the ovary. On the style of plants with a strong phenotype, protrusions ranged from conical cells to long-stalked trichomes (Fig. 4e). On the stamen filament of transgenic flowers, short trichomes <30 μm in length were the most common type of protrusion. The anther of wild-type flowers has a regular arrangement of conical cells (Fig. 4f). In all transgenic lines, epidermal cells had an altered shape and distinct bulbous tip (Fig. 4g). For some cells, the tips

of cells were extended into trichomes of varying lengths.

At the tip of the corolla, the epidermis of wild-type flowers has a regular arrangement of conical cells with a pronounced bulb at the tip of each cell (Fig. 4h). In all lines expressing 35S:*CcSBG9A1*, epidermal cell shape was more variable particularly at the tips of cells, which protruded to varying degrees (Fig. 4i). Multicellular trichomes >50 μm in length, and sometimes glandular, were found to be sparsely distributed amongst the conical cells.

On the adaxial epidermis of wild-type leaves, cells are largely flat with a rounded base shape. Long multicellular trichomes, and shorter hydathode-type trichomes, are irregularly distributed on the leaf epidermis (Fig. 4j). In several transgenic lines, some of the long multicellular trichomes had multiple branches (Fig. 4k). Between these trichomes the epidermal cells remained largely flat or lenticular, but many of these cells developed a distinct peak or tip (Fig. 4k). Occasionally, these cells also had an altered overall shape and were distinctly conical. No changes in epidermal morphology were observed on the abaxial leaf epidermis of transgenic lines.

Ontogeny of tepal epidermal outgrowth in Cabomba caroliniana

Tepal epidermal morphology was characterised at five developmental stages of *C. caroliniana*: (1) 1 mm buds, (2) 2 mm buds, (3) 4 mm buds, (4) 5 mm buds, and (5) 7 mm buds or flowers at anthesis. Flowers of *Cabomba* have whorled floral phyllotaxy, with two whorls of three petaloid tepals forming in alternating positions (Fig. 5a). The inner tepals are developmentally retarded with respect to the outer tepals and other floral organs, and thus for each stage the tepals from the inner and outer whorls were imaged separately (Vialette-Guiraud *et al*., 2011). Specific zones along the length of the tepal were identified for comparative analysis, as outlined in Fig. 5a.

At the youngest stage (stage 1), the inner and outer whorls of tepals were indistinguishable, and there was no evidence of cell outgrowth (Fig. 5b). By stage 2, nectaries are present towards the base of the inner tepals, although these are restricted to the very outer edges of the tepal (Fig. 5c). Cells at the tip of the tepal are similar in appearance in inner and outer tepal whorls (Fig. 5d), while those at the base of the tepal are more variable. There was no evidence of cell outgrowth. By stage 3, pronounced conical cells are visible at the tip of both the inner and outer tepals. On the inner tepals these cones have a more pointed shape (Fig. 5e), while they are distinctly rounded on the outer whorl. At the base of the inner tepal, nectaries are well developed (Fig. 5f). Stage 4 shares an almost identical phenotype with

stage 3 (Fig. 5g, 5h). By stage 5, conical epidermal cells at the tips of the tepals are more uniform, but there is no change in their total degree of protrusion (Fig. 5i, 5j).

Expression analyses of CcSBG9A1 *in* Cabomba caroliniana

Quantitative RT-PCR was used to determine whether expression levels of *CcSBG9A1* correlated with conical cell development in *C. caroliniana*. Expression analyses were conducted across a range of floral tissues – tepals (pooled inner and outer whorls), stamens and carpels – and three developmental stages (pooled bud stages 1 and 2 (less then 3mm), pooled bud stages 3 and 4 (3-5mm in length), and bud stage 5 (more than 5mm in length). Mean expression values for each tissue and developmental stage were calculated relative to expression levels of *CcActin* from three technical and three biological replicates (Fig. 5k). The highest level of *CcSBG9A1* expression was in young tepals at stages 1 and 2, immediately prior to the appearance of conical cells (at stage 3). There were very low levels of *CcSBG9A1* expression in tepals larger than 3 mm and in mature flowers (>5 mm). A *t*-test confirmed that *CcSBG9A1* expression in the tepals of <3 mm buds is significantly higher than in the tepals of >5 mm buds ($t(4) = 5.92$, $P < 0.01$). When *CcSBG9A1* expression is compared in the different tissues of <3 mm buds, it is significantly higher in the tepals relative to the stamens ($t(4) = 6.37$, $P < 0.01$) or carpels ($t(4) = 6.12$, $P < 0.01$).

Discussion

Conical tepal epidermal cells are present in several ANA-grade angiosperms

Our examination of species from the three ANA-grade orders (Fig. 2) reveals complex tepal surfaces in ANA-grade species, consistent with the diversity of flower structure in these taxa which contributes to the bigger picture of perianth epidermal morphology evolution across the angiosperms. Tepal surfaces are rarely entirely uniform, and can differ on the same flower and even on the same tepal. Two ANA-grade genera, *Cabomba* and *Austrobaileya*, possess distinctly conical cells over most of the adaxial tepal surface. In several other ANA-grade genera (e.g. *Kadsura*, *Victoria*), cells are conical or subconical on some parts of the tepal surface. *Amborella trichopoda*, the putative sister to all other angiosperms, possesses strongly domed cells. In contrast, a few ANA-grade species possess mostly flat cells on the tepal surface (e.g. *Nuphar*, *Trimenia*).

The conical-papillate petal epidermis represents the most common type in

angiosperms (Kay *et al*., 1981), but there also exist many subconical types with a rounded or flattened apex, as we have found in *Amborella* and *Kadsura*. The widespread distribution of conical or subconical cells in all three ANA-grade lineages indicates that the capacity to produce them is of ancient origin. Few studies have examined the apparently simple transition from a lenticular or subconical cell to a conical cell. In many eudicots, formation of both conical cells and trichomes on the petal epidermis is determined by SBG9A MYB transcription factors (Martin *et al*., 2002. Perez-Rodriguez *et al*., 2005). Ectopic expression of SBG9A MYB genes can induce both conical and lenticular cellular outgrowth (Martin *et al.*, 2002; Jaffe *et al.*, 2007). In some eudicots there is clear evidence for an evolutionary loss of the conical cell form within a specific taxonomic group or natural community (e.g. Ojeda *et al.*, 2009, Ojeda *et al.*, 2016).

Pollination biology is also diverse among ANA-grade species, though data are relatively sparse for some taxa (Thien *et al.*, 2009; Endress, 2010; Luo *et al.*, 2018). Beetle pollination is common in the waterlily family Nymphaeaceae and in some Schisandraceae; flies are the major pollinators of *Austrobaileya* and *Illicium*, and Schisandraceae are predominantly pollinated by nocturnal gall midges (Endress, 2010; Luo *et al.*, 2018). Petal surfaces with domed and/or conical cells are frequently involved in scent production (Vogel, 1990). The tiny white flowers of *Amborella* produce a scent that attracts nocturnal moths and other insects (Thien *et al*., 2009). A likely source for the scent is the prominent regions of the central part of the tepal surface, which function as osmophores. The waterlily genus *Cabomba*, which possesses prominent conical cells, is unusual among ANA-grade angiosperms in possessing well-defined nectaries on the surfaces of the inner tepals; the nectar provides a reward to visiting pollinating insects such as bees, wasps and flies (Schneider and Jeter, 1982; Taylor and Williams, 2009; Vialette-Guiraud *et al.*, 2011; Luo *et al.*, 2018). Two genera that lack conical cells are probably abiotically pollinated: *Trithuria* (Hydatellaceae) and *Brasenia* (Cabombaceae), supporting a correlation between conical cells and pollinator attraction.

An SBG9A MYB transcription factor from an early diverging angiosperm can induce ectopic conical cell development

To analyse the homologies of conical tepal epidermal cells, we explored the developmental genetic processes underpinning cellular differentiation. A common developmental programme could suggest a single ancestral origin followed by repeated evolutionary losses or modifications. The SBG9A MYB transcription factors are known to control petal

epidermal cell outgrowth in both eudicots (Noda *et al.*, 1994; Machado *et al*., 2009; Di Stilio *et al.*, 2009; Brockington *et al*., 2013) and monocots (Gilding and Marks, 2010). We therefore examined whether this subgroup of *MYB* genes could perform similar functions in ANA-grade angiosperms, suggesting a single origin of conical cells.

Analyses of SBG9A MYB protein function are sometimes hampered by the many duplications seen within the gene family at different phylogenetic levels (Bedon *et al.*, 2014). However, our phylogenetic reconstruction, coupled with evidence from published transcriptomes, demonstrates only a single SBG9A gene in the *Cabomba* genome. The gene family is divided into MIXTA and MIXTA-like clades following a duplication at the base of the eudicots (Brockington *et al.*, 2013), but the ANA-grade members form a clade that diverged before this duplication (Fig. 2). Furthermore, although there are lineage-specific duplications in some genera within this clade, we found no evidence for a deep duplication event within the ANA-grade lineages.

Ectopic expression of *CcSBG9A1* in tobacco revealed that the protein has the ability to induce anisotropic cell expansion and cellular outgrowth in all tissues tested, indicating that it is able to induce cellular differentiation alone (or with a ubiquitously expressed partner). The strength of the ectopic expression phenotype is remarkable. The same heterologous approach using the same strong constitutive promoter (double copy of the 35S promoter from CaMV) in *N. tabacum* has been used for several other angiosperm SBG9A MYB genes over the last 20 years. This list includes *TtMYBML2* from the basal eudicot *Thalictrum thaloctroides* (Di Stilio *et al*., 2009), *AtMYB16, AtMYB106* from *Arabidopsis* (Baumann *et al*., 2007; Gilding and Marks, 2010), *PhMYB1* from *Petunia hybrida* (Baumann *et al*., 2007), and the four SBG9-A genes in *Antirrhinum majus* (*AmMIXTA, AmMIXTA-LIKE 1*, *AmMIXTA-LIKE2* and *AmMIXTA-LIKE 3*) (Glover *et al*., 1998; Perez-Rodriguez *et al*., 2005; Baumann *et al*., 2007; Jaffé *et al*., 2007). It is notable that *CcSBG9A1* induces a much stronger phenotype than most previously characterized SBG9A MYB genes in this bioassay. For example, *PhMYB1*, *AmMYBML2*, *AtMYB16* and *TtMYBML2* share similar expression patterns and similar phenotypes when ectopically expressed in tobacco. Transgenic tobacco plants exhibit ectopic outgrowths on the surface of the ovary, as well as an increase in the height and change in shape of conical cells on the corolla. However, these outgrowths never develop into multicellular trichomes, and no changes were observed to the other floral organs, or vegetative leaves (some changes were observed on inflorescence leaves) (Di Stilio *et al*., 2009; Baumann *et al*., 2007). The strongest reported phenotypes from this bioassay are for *N. tabacum* plants overexpressing *AmMIXTA*, which exhibit long multicellular trichomes

on the ovary and at the tip of the inner corolla. On the leaves, several parallels can be drawn with the effects of *CcSBG9A1* expression. For example, the majority of cells on the adaxial leaf epidermis have a single, central outgrowth. These outgrowths are almost identical on the adaxial leaf epidermis of transgenic tobacco expressing 35S:*CcSBG9A1* and 35S:*AmMIXTA*. Long-stalked, multicellular branched trichomes were also observed on the adaxial leaf epidermis of both transgenic lines (Glover *et al*., 1998; Perez-Rodriguez *et al*., 2005). Phenotypic strength may be affected by position of transgene insertion and transgene expression level, so our conclusions here must be tentative, but it is nonetheless notable that the phenotypes observed in this study are consistently stronger than those for most related genes using the same bioassay system.

The four SBG9A genes in *A. majus* have arisen from Antirrhineae-specific duplication events within the MIXTA (*AmMIXTA* and *AmMIXTA-LIKE 1*) and MIXTA-like (*AmMIXTA-LIKE2* and *AmMIXTA-LIKE 3*) clades. These four genes show sequence homology and may have overlapping functions, but they are not functionally redundant. It has been suggested that formation of fully developed conical cells on the petals of *A. majus* requires two distinct activities. For example, *AmMIXTA* and *AmMYBML1* may be responsible for initiating conical cell development, while *AmMYBML2* and *AmMYBML3* coordinate a second stage of elongation that leads to a complete cone (Perez-Rodriguez *et al*., 2005).

Our study shows that the gene duplication event that led to formation of the MIXTA and MIXTA-like clades, as well as the Antirrhineae-specific duplication event that gave rise to *AmMYBML1*, *2* and *3*, arose after the divergence of *Cabomba* (Fig. 2). There is no evidence of an ancient gene duplication event in the MIXTA and MIXTA-like clades within either the early diverging angiosperm or the early land-plant lineages. In turn, we infer that the single CcSBG9A1 protein plays a crucial role in inducing anisotropic cell expansion and coordinating conical cell development in *C. caroliniana*. The ability of *CcSBG9A1* to induce the formation of ectopic cell outgrowths in tobacco indicates that the encoded CcSBG9A1 protein is capable of regulating similar transcriptional targets as other members of the SBG9A lineage. The strength of the phenotype suggests that CcSBG9A1 is a particularly effective transcriptional regulator of the downstream cellular differentiation pathway and has the potential to act as a master regulator of epidermal cell outgrowth.

A SBG9A MYB transcription factor is expressed specifically in developing tepals of Cabomba caroliniana, immediately prior to conical cell outgrowth

Since it is not possible to transform *Cabomba caroliniana*, we sought additional correlative evidence in support of a role for *CCSBG9A1* in conical cell development. Although CcSBG9A1 is clearly able to induce cellular outgrowth, its native phenotypic effects will depend on the transcriptional profile of the gene encoding it. We used an ontogenetic series to determine that epidermal cell outgrowth in the *Cabomba* tepal occurs at growth stage 3, when buds are between 2 and 4mm long. We predicted that the transcriptional regulator controlling cellular outgrowth would be expressed in earlier stages of tepal development. Quantitative RT-PCR analyses of dissected tissues revealed that *CcSBG9A1* is most strongly expressed in tepals of buds below 3mm in length. Transcript is almost undetectable in other floral organs (stamens and carpels) and in tepals at later developmental stages when the conical cells are already present. This expression pattern correlates strongly with a role in regulating conical tepal epidermal cell development.

Conclusions

Our study clearly demonstrates the presence of conical perianth epidermal cells in some of the earliest surviving angiosperm lineages. Our combined strong, if correlative, evidence suggests that outgrowth of the conical cells in *Cabomba* is regulated by the same MYB SBG9A-initiated pathway that regulates petal cell development in eudicots. This ancient origin for conical cells and their developmental programme suggests that the many angiosperm species that lack conical petal cells represent secondary losses of an ancestral character. We hypothesise that changes in *cis*-regulation or protein function of *SBG9* MYB genes, potentially correlated with shifts in pollinator type and behavior, are responsible for the repeated loss of conical cells in many lineages.

Supplementary Data

The following Supplementary Data are available for this article:

Figure S1. Genotyping transgenic tobacco lines expressing *CcSBG9A-1*.

Figure S2. Maximum likelihood phylogram of SBG9A *MYB* genes from seed plants.

Table S1. Primer sequences

Acknowledgements

We thank Matthew Dorling for excellent plant care, Alex Summers and Cambridge University Botanic Garden for help with *Cabomba* cultivation, and Carlos Magdalena and other staff of the Royal Botanic Gardens Kew for living and spirit material. We thank Richard Bateman, Carlos Magdalena, Edwige Moyroud and Charlie Scutt for helpful discussions. AR was supported by a Biotechnology and Biological Sciences Research Council (BBSRC) doctoral training grant (DTG) studentship.

Author contributions

The study was designed by BJG and PJR. BJG wrote the manuscript, with input from all authors. Electron microscopy was performed by AR and PJR, molecular biology by AR, and phylogenetic analyses by SFB.

Data availability

The sequence of *CcSBG9A1* has been submitted to the GenBank database under accession number ON364012. All materials available on request from BJG.

References

Alcorn K, Whitney H, Glover B. 2012. Flower movement increases pollinator preference for flowers with better grip. Functional Ecology **26,** 941–947.

Angiosperm Phylogeny Group [APG] **III**. 2009. An update of the Angiosperm Phylogeny Group classification for the orders and families of flowering plants. Botanical Journal of the Linnean Society **161,** 105–121.

Baumann K, Perez-Rodriguez M, Bradley D, Venail J, Bailey P, Jin H, Koes R, Roberts K, Martin C. 2007. Control of cell and petal morphogenesis by R2R3 MYB transcription factors. Development **134,** 1691–1701.

Bedon F, Ziolkowski L, Walford SA, Dennis ES, Llewellyn DJ. 2014. Members of the MYB MIXTA-like transcription factors may orchestrate the initiation of fiber development in cotton seeds. Frontiers in Plant Science **5,** 179.

Brockington SF, Alvarez-Fernandez R, Landis JB, Alcorn K, Walker RH, Thomas MM, Hileman LC, Glover BJ. 2013. Evolutionary analysis of the MIXTA gene family highlights potential targets for the study of cellular differentiation. Molecular Biology and Evolution **30,** 526–540.

Christensen KI, Hansen H V. 1998. SEM-studies of epidermal patterns of petals in the angiosperms. Copenhagen: Council for Nordic Publications in Botany.

Coiro M, Barone Lumaga MR. 2018. Disentangling historical signal and pollinator selection on the micromorphology of flowers: an example from the floral epidermis of the Nymphaeaceae. Plant Biology **20,** 902–915.**Di Stilio VS, Martin C, Schulfer AF, Connelly CF**. 2009. An ortholog of *MIXTA-like2* controls epidermal cell shape in flowers of

Thalictrum. New Phytologist **183,** 718–728.

Dubos C, Stracke R, Grotewold E, Weisshaar B, Martin C, Lepiniec L. 2010. MYB transcription factors in Arabidopsis. Trends in Plant Science **15,** 573–581.

Dyer AG, Whitney HM, Arnold SEJ, Glover BJ, Chittka L. 2007. Mutations perturbing petal cell shape and anthocyanin synthesis influence bumblebee perception of *Antirrhinum majus* flower colour. Arthropod-Plant Interactions **1,** 45–55.**Endress PK.** 2008. Perianth biology in the basal grade of extant angiosperms. International Journal of Plant Science **169,** 844–862.

Endress PK. 2010. The evolution of floral biology in basal angiosperms. Philosophical Transactions of the Royal Society B. Biological Science **365,** 411–421.

Endress PK. 2011 Evolutionary diversification of the flowers in angiosperms. American Journal of Botany **98,** 370–396.

Gilding EK, Marks MD. 2010. Analysis of purified glabra3-shapeshifter trichomes reveals a role for NOECK in regulating early trichome morphogenic events. The Plant Journal **64,** 304–317.

Glover BJ, Martin C. 1998. The role of petal cell shape and pigmentation in pollination success in *Antirrhinum majus*. Heredity **80,** 778–784.

Glover BJ, Perez-Rodriguez M, Martin C. 1998. Development of several epidermal cell types can be specified by the same MYB-related plant transcription factor. Development **125,** 3497–3508.

Gorton HL, Vogelmann TC. 1996. Effects of epidermal cell shape and pigmentation on optical properties of *Antirrhinum* petals at visible and ultraviolet wavelengths. Plant Physiology **11,** 879–888.

Hellens RP, Edwards EA, Leyland NR, Bean S, Mullineaux PM. 2000. pGreen: a versatile and flexible binary Ti vector for Agrobacterium-mediated plant transformation. Plant Molecular Biology **42,** 819–832.

Horsch RB, Fry JE, Hoffman NL, Eichholtz D, Rogers SG, Fraley RT. 1985. A simple and general method for transferring genes into plants. Science **227,** 1229–1231.

Jaffe FW, Tattersall A, Glover BJ. 2007. A truncated MYB transcription factor from *Antirrhinum majus* regulates epidermal cell outgrowth. Journal of Experimental Botany **58,** 1515–1524.

Kay QON, Daoud HS, Stirton CH. 1981. Pigment distribution, light reflection and cell structure in petals. Botanical Journal of the Linnean Society **83,** 57–83.

Kevan PG. 1999. Pollinators as bioindicators of the state of the environment: species, activity and diversity. Agriculture Ecosystems and Environment **74,** 373–393.

Kevan PG, Baker HG. 1983. Insects as flower visitors and pollinators. Annual Review of Entomology **28,** 407–453.

Kevan PG, Lanet MA. 1985. Flower petal microtexture is a tactile cue for bees. Ecology **82,** 4750–4752.

Klein AM, Vaissière BE, Cane JH, Steffan-Dewenter I, Cunningham SA, Kremen C, Tscharntke T. 2007. Importance of pollinators in changing landscapes for world crops. Proceedings of the Royal Society B **274,** 303–313.

Luo S-X, Zhang L-J, Yuan S, Ma Z-H, Zhang D-X, Renner SS. 2018 The largest early-diverging angiosperm family is mostly pollinated by ovipositing insects and so are most surviving lineages of early angiosperms. Proceedings of the Royal Society B: Biological Sciences **285,** 20172365.

Machado A, Wu Y, Yang Y, Llewellyn DJ, Dennis ES. 2009. The MYB transcription factor GhMYB25 regulates early fibre and trichome development. The Plant Journal **59,** 52–62.

Martin C, Paz-Ares J. 1997. MYB transcription factors in plants. Trends in Genetics **13,** 67–73.

Martin C, Bhatt K, Baumann K, Jin H, Zachgo S, Roberts K, Schwarz-Sommer Z, Glover B, Perez-Rodrigues M. 2002. The mechanics of cell fate determination in petals. Philosophical Transactions of the Royal Society, London B **357,** 809–813.

Mathews S, Donoghue MJ. 1999. The root of angiosperm phylogeny inferred from duplicate phytochrome genes. Science **286,** 947–950.

Noda K, Glover BJ, Linstead P, Martin C. 1994. Flower colour intensity depends on specialized cell shape controlled by a MYB-related transcription factor. Nature **369,** 661–664.

Ojeda I, Francisco-Ortega J, Cronk QCB. 2009. Evolution of petal epidermal micromorphology in Leguminosae and its use as a marker of petal identity. Annals of Botany **104,** 1099–1110.

Ojeda DI, Valido A, Fernández de Castro AG, Ortega-Olivencia A, Fuertes-Aguilar J, Carvalho JA, Santos-Guerra A. 2016. Pollinator shifts drive petal epidermal evolution on the Macaronesian Islands bird-flowered species. Biology Letters **12,** 20160022.

Parkinson CL, Adams KL, Palmer JD. 1999. Multigene analyses identify the three earliest lineages of extant flowering plants. Current Biology **9,** 1485–1488.

Perez-Rodriguez M, Jaffe FW, Butelli E, Glover BJ, Martin C. 2005. Development of three different cell types is associated with the activity of a specific MYB transcription factor in the ventral petal of *Antirrhinum majus* flowers. Development **132,** 359–370.

Rands SA, Glover BJ, Whitney HM. 2011. Floral epidermal structure and flower orientation: getting to grips with awkward flowers. Arthropod-Plant Interactions **5,** 279–285.

Romanov MS, Bobrov AVFC, Endress PK. 2013. Structure of the unusual explosive fruits of the early diverging angiosperm *Illicium* (Schisandraceae *s.l.* , Austrobaileyales). Botanical Journal of the Linnean Society **171,** 640–654.

Rudall PJ, Sokoloff DD, Remizowa MV, Conran JG, Davis JI, Macfarlane TD, Stevenson DW. 2007. Morphology of Hydatellaceae, an anomalous aquatic family recently recognized as an early-divergent angiosperm lineage. American Journal of Botany **94,** 1073–1092.

Schiestl FP, Johnson SD. 2013. Pollinator-mediated evolution of floral signals. Trends in Ecology and Evolution **28,** 307–315.

Schneider EL, Jeter JM. 1982. Morphological studies of the Nymphaeaceae. XII. The floral biology of *Cabomba caroliniana*. American Journal of Botany **69,** 1410–1419.

Taneda H, Watanabe-Taneda A, Chhetry R, Ikeda H. 2015. A theoretical approach to the relationship between wettability and surface microstructures of epidermal cells and structured cuticles of flower petals. Annals of Botany **115,** 923–937.

Taylor ML, Williams JH. 2009. Consequences of pollination syndrome evolution for post-pollination biology in an ancient angiosperm family. International Journal of Plant Sciences **170,** 584–598.

Thien LB, Bernhardt P, Devall MS, Chen Z-D, Luo Y-B, Fan J-H, Yuan L-C, Williams JH. 2009. Pollination biology of basal angiosperms (ANITA grade). American Journal of Botany **96,** 166–182.

Vialette-Guiraud ACM, Alaux M, Legeai F, Finet C, Chambrier P, Brown SC, Chauvet

A, Magdalena C, Rudall PJ, Scutt CP. **2011**. *Cabomba* as a model for studies of early angiosperm evolution. Annals of Botany **108,** 589–98.

Vogel S. 1990. The role of scent glands in pollination. New Delhi: Amerind Publishing company.

Warner KA, Rudall PJ, Frohlich MW. 2008. Differentiation of perianth organs in Nymphaeales. Taxon **57,** 1096–1109.

Warner KA, Rudall PJ, Frohlich MW. 2009. Environmental control of sepalness and petalness in perianth organs of waterlilies: a new Mosaic Theory for the evolutionary origin of a differentiated perianth. Journal of Experimental Botany **60,** 3559–3574.

Whitney HM, Chittka L, Bruce TJA, Glover BJ. 2009. Conical epidermal cells allow bees to grip flowers and increase foraging efficiency. Current Biology **19,** 948–953.

Zini LM, Galati BG, Ferrucci MS. 2017. Perianth organs in Nymphaeaceae: comparative study on epidermal and structural characters. Journal of Plant Research **130,** 1047–1060.

Table 1. *Species and material examined*

Family	Species examined	Material examined*
Amborellaceae	*Amborella trichopoda* Baill.	HK: *s.n.*
Nymphaeaceae	*N. odorata* Aiton subsp. *tuberosa* Wiersema & Hellq.	HK: 1969-19765
	N. violacea Lehm.	HK: 2007-1810
	Victoria cruziana Orbign.	HK: 2011-1436
Cabombaceae	*C. caroliniana* A.Gray	HK: *s.n.* and commercial source (living plants)
	C. furcata Schult. & Schult.f	Commercial source (living plants)
Austrobaileyaceae	*Austrobaileya scandens* C.T.White	HK: 2012-464
Schisandraceae	*Kadsura heteroclite* Craib.	HK: 1985-4488
	K. japonica Benth.	HK: 1989-3952
	Schisandra rubriflora Rehder & E.H.Wilson	HK: 1969-19804
Illiciaceae	*Illicium floridanum* J.Ellis	HK: 2011-880
	I. simonsii Maxim.	HK: 1994-3682
Trimeniaceae	*Trimenia moorei* (Oliv.) Philipson	*s.n.*

*****HK indicates material cultivated at RBG Kew. *s.n.* indicates accession number absent

Species	Tepal surface morphology	Data source
Amborellaceae		
Amborella trichopoda	Distinct conical cells absent, but cells strongly domed (subconical) and either smooth or with a flattened tip with fine surface ridges (Fig. 1A–C).	This paper
Cabombaceae		
Brasenia schreberi	Conical cells absent; cells mostly flat and surfaces smooth; occasional long trichomes present.	Warner *et al*. (2008)
Cabomba caroliniana; *C. furcata*	Distinct conical cells present except at tepal bases, where cells are mostly flat (Fig. 1D–F).	This paper
Hydatellaceae		
Trithuria spp.	Conical cells absent; cells flat and surfaces smooth.	Rudall *et al*. (2007, 2009)
Nymphaeaceae		
Euryale ferox	Conical cells absent; cells flat or slightly domed.	Coiro and Barone Lumaga (2018)
Nymphaea caerulea; N. odorata subsp. *tuberosa*; *N. Violacea; N.* spp.	Conical cells absent; cells flat or slightly domed. Cell surfaces smooth (*N. odorata* subsp. *tuberosa*) or with numerous small lumps (micropapillae) on each cell (*N. violacea,* Fig. 1G, H).	This paper; Warner *et al*. (2008, 2009); Coiro and Barone Lumaga (2018)
Nuphar lutea	Conical cells absent; cells flat and smooth.	Warner *et al*., 2008, 2009); Coiro and Barone Lumaga (2018)
Victoria cruziana	Conical cells absent from outer tepals but present on the inner staminoid tepals, where they possess a pronounced bulb at the tip, surrounded by radiating striations (Fig. 1I). Surfaces of other tepals with cells domed and smooth.	This paper; Coiro and Barone Lumaga (2018)
Austrobaileyaceae		
Austrobaileya scandens	Conical cells present on most flower parts (Fig. 1J–L), especially the inner tepals, stamens and staminodia, always with fine radiating striations. Outer tepals with	This paper

	relatively flat cells, except towards margins, where shallow conical cells present.	
Illiciaceae		
Illicium simonsii, I. floridanum	Distinctly conical cells absent, but cells range from shallowly domed at the tepal base to more strongly domed towards tepal apex, especially in *I. simonsii*. Clear striations present on surfaces of most cells, either axially oriented or chaotic (Fig. 1M–O).	This paper
Schisandraceae		
Kadsura heteroclita, K. japonica	Distinctly conical cells occasionally present; cells ranging from flat to strongly domed or subconical, sometimes with an inflated tip (Fig. 1R, S). Surfaces relatively smooth or with fine nanoridges.	This paper
Schisandra rubriflora	Conical cells absent; cells mostly flat or slightly domed (Fig. 1P, Q). Surfaces with an irregular pattern of shallow cuticular nanoridges.	This paper
Trimeniaceae		
Trimenia moorei	Conical cells absent; cells mostly flat or slightly domed (Fig. 1T). Surfaces smooth or with axially oriented cuticular striations present. Central region of abaxial epidermis with long unicellular trichomes.	This paper

Table 2: *Morphology of the adaxial epidermis of tepals in ANA-grade families*

Figure Legends

Figure 1. Relationships of the major angiosperm clade (APG III, 2009), highlighting the ANA-grade lineages analysed in this paper.

Figure 2. Adaxial epidermal morphology of coloured (insect-attracting) organs in ANA-grade flowers (photos and SEMs). A–C. *Amborella trichopoda*, entire tepal showing central bulbous regions (arrowed) in (B) and detail of tepal surface showing domed flat-topped cells with chaotic surface patterning in (B). D, E. *Cabomba caroliniana*, tepal surface at junction between flat-celled base (right) and mid-region with conical cells (left) in (E). F. detail of tepal surface of *Cabomba furcata* with conical cells. G, H. *Nymphaea violacea*, detail of inner tepal surface in (H). I. *Victoria cruziana*, detail of inner tepal surface showing cells with central prominence and radiating striations. J–L. *Austrobaileya scandens*, details of inner tepal surface near margin (K), and staminode surface (L), both showing conical cells with fine striations. M–O. *Illicium simonsii*, details of (N) mid region of tepal showing cells with central prominence and chaotic striations, and (O) base of tepal showing flat cells with chaotic striations. P, Q. *Schisandra rubriflora*, detail of tepal surface showing flat cells in (Q). R, S. *Kadsura heteroclita*, detail of tepal surface showing domed cells in (S). T. *Trimenia moorei*, detail of tepal surface showing flat cells. Scale bars = 20 µm, except in (E) = 100 µm, in (H) = 50 µm, in (I) and (Q) = 10 µm.

Figure 3. Maximum likelihood phylogram of SBG9A *MYB* genes from seed plants. SH support values are reported on the tree topology. The MIXTA and MIXTA-like clades of eudicot family members are marked. *CcSBG9A1* is highlighted in red.

Figure 4. Ectopic expression of *CcSBG9A1* in tobacco. A. Wild type (left) and transgenic (centre, right) flowers. B. SEM image of wild type tobacco carpel epidermis. C. SEM image of tobacco carpel expressing *CcSBG9A1*. D. SEM image of wild type tobacco style epidermis. E. SEM image of tobacco style expressing *CcSBG9A1*. F. SEM image of wild type tobacco anther head. G. SEM images of anther heads of 2 independent tobacco lines expressing *CcSBG9A1*. H. SEM image of wild type tobacco petal epidermis. I. SEM images of petals of 2 independent tobacco lines expressing *CcSBG9A1*. J. SEM image of wild type tobacco leaf adaxial epidermis. K. SEM images of adaxial leaf epidermis of 2 independent tobacco lines expressing *CcSBG9A1*. All scale bars = 50µm.

Figure 5. Development of conical tepal epidermal cells in *Cabomba caroliniana.* A. Schematic diagram showing the tepal morphology of *Cabomba* as used for the SEM developmental series. Carpels and stamens are not shown. The positions of the inner and outer tepal whorls (see key), nectaries, and sampling zones (1-3) are marked. B. SEM image of adaxial tepal epidermis at stage 1, zone C. Inner and outer tepals are indistinguishable at this stage. C. SEM image of adaxial epidermis of inner tepal at stage 2, zone C. D. SEM image of adaxial epidermis of outer tepal at stage 2, zone A. E. SEM image of adaxial epidermis of inner tepal at stage 3, zone A. F. SEM image of adaxial epidermis of outer tepal at stage 3, zone C. G. SEM image of adaxial epidermis of inner tepal at stage 4, zone A. H. SEM image of adaxial epidermis of outer tepal at stage 4, zone A. I. SEM image of adaxial epidermis of inner tepal at stage 5, zone A. J. SEM image of adaxial epidermis of outer tepal at stage 5, zone A. K. qRT-PCR analysis of *CcSBG9A-1* expression in different tissues and at different developmental stages (<3mm = stages 1+2; 3-5mm = stages 3+4; >5mm = stage 5;) of *Cabomba caroliniana*. Target gene expression was quantified relative to actin. Values represent mean expression values and standard errors (n = 3). All scale bars = 20μm.

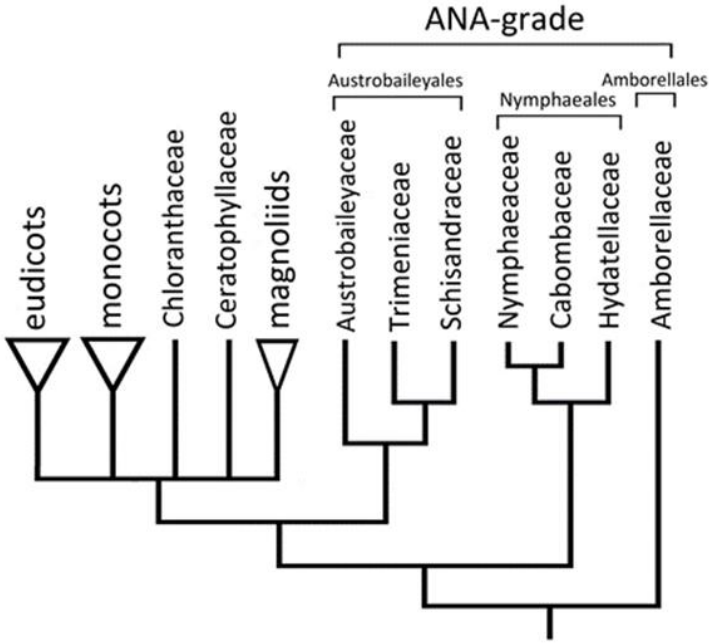
ANA-grade
Austrobaileyales
Amborellales
Nymphaeales
eudicots
monocots
Chloranthaceae
Ceratophyllaceae
magnoliids
Austrobaileyaceae
Trimeniaceae
Schisandraceae
Nymphaeaceae
Cabombaceae
Hydatellaceae
Amborellaceae

FIGURE 1.

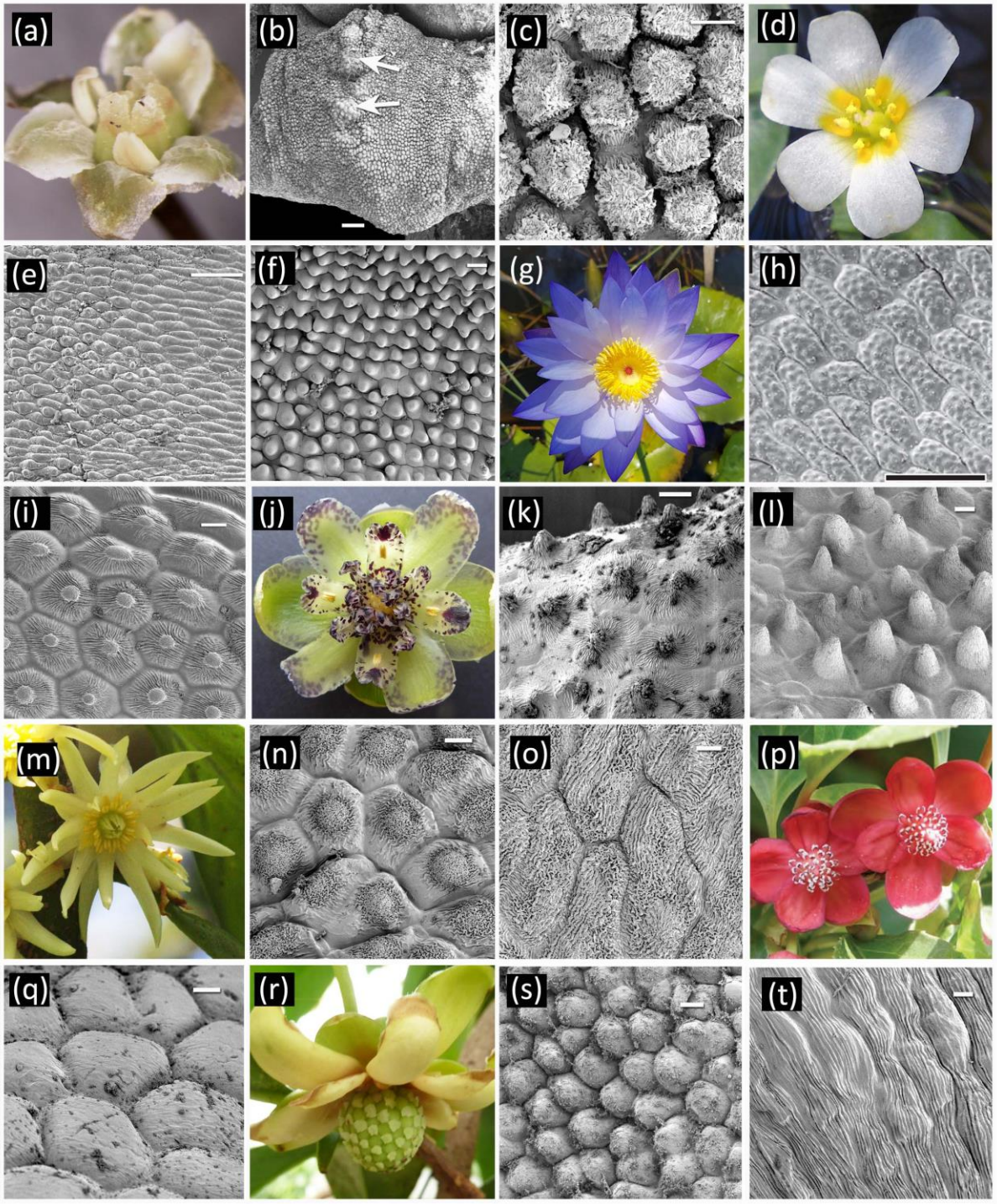

FIGURE 2

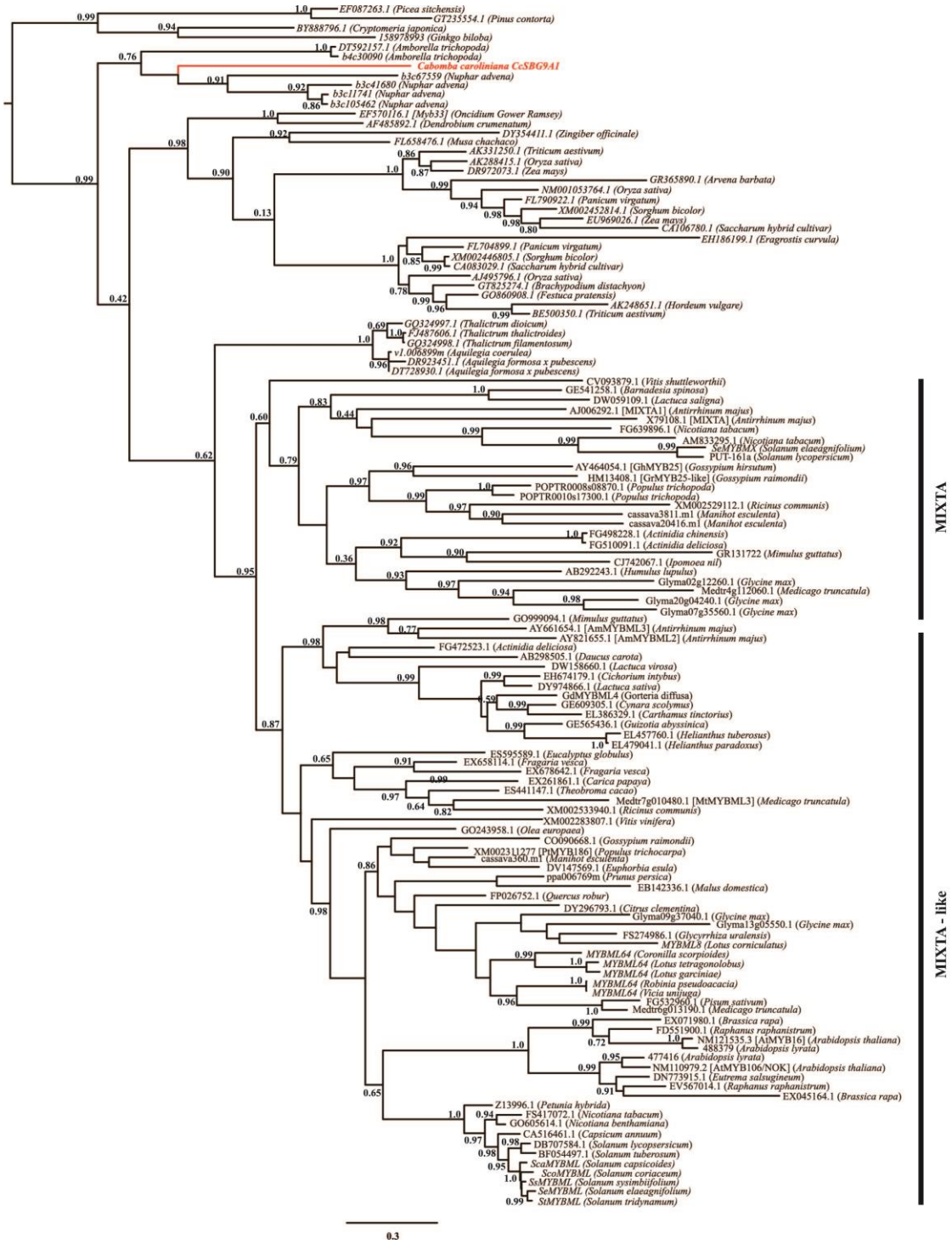
EF087263.1 (Picea sitchensis)
GT235554.1 (Pinus contorta)
BY888796.1 (Cryptomeria japonica)
158978993 (Ginkgo biloba)
DT592157.1 (Amborella trichopoda)
b4c30090 (Amborella trichopoda)
Cabomba caroliniana CcSBG9A1
b3c67559 (Nuphar advena)
b3c41680 (Nuphar advena)
b3c11741 (Nuphar advena)
b3c105462 (Nuphar advena)
EF570116.1 [Myb33] (Oncidium Gower Ramsey)
AF485892.1 (Dendrobium crumenatum)
DY354411.1 (Zingiber officinale)
FL658476.1 (Musa chachaco)
AK331250.1 (Triticum aestivum)
AK288415.1 (Oryza sativa)
DR972073.1 (Zea mays)
GR365890.1 (Arvena barbata)
NM001053764.1 (Oryza sativa)
FL790922.1 (Panicum virgatum)
XM002452814.1 (Sorghum bicolor)
EU969026.1 (Zea mays)
CA106780.1 (Saccharum hybrid cultivar)
EH186199.1 (Eragrostis curvula)
FL704899.1 (Panicum virgatum)
XM002446805.1 (Sorghum bicolor)
CA083029.1 (Saccharum hybrid cultivar)
AJ495796.1 (Oryza sativa)
GT825274.1 (Brachypodium distachyon)
GO860908.1 (Festuca pratensis)
AK248651.1 (Hordeum vulgare)
BE500350.1 (Triticum aestivum)
GO324997.1 (Thalictrum dioicum)
FJ487606.1 (Thalictrum thalictroides)
GO324998.1 (Thalictrum filamentosum)
v1.006899m (Aquilegia coerulea)
DR923451.1 (Aquilegia formosa x pubescens)
DT728930.1 (Aquilegia formosa x pubescens)
CV093879.1 (Vitis shuttleworthii)
GE541258.1 (Barnadesia spinosa)
DW059109.1 (Lactuca saligna)
AJ006292.1 [MIXTA1] (Antirrhinum majus)
X79108.1 [MIXTA] (Antirrhinum majus)
FG639896.1 (Nicotiana tabacum)
AM833295.1 (Nicotiana tabacum)
ScMYBMX (Solanum elaeagnifolium)
PUT-161a (Solanum lycopersicum)
AY464054.1 [GhMYB25] (Gossypium hirsutum)
HM13408.1 [GrMYB25-like] (Gossypium raimondii)
POPTR0008s08870.1 (Populus trichopoda)
POPTR0010s17300.1 (Populus trichopoda)
XM002529112.1 (Ricinus communis)
cassava3811.m1 (Manihot esculenta)
cassava20416.m1 (Manihot esculenta)
FG498228.1 (Actinidia chinensis)
FG510091.1 (Actinidia deliciosa)
GR131722 (Mimulus guttatus)
CJ742067.1 (Ipomoea nil)
AB292243.1 (Humulus lupulus)
Glyma02g12260.1 (Glycine max)
Medtr4g112060.1 (Medicago truncatula)
Glyma20g04240.1 (Glycine max)
Glyma07g35560.1 (Glycine max)
MIXTA
GO999094.1 (Mimulus guttatus)
AY661654.1 [AmMYBML3] (Antirrhinum majus)
AY821655.1 [AmMYBML2] (Antirrhinum majus)
FG472523.1 (Actinidia deliciosa)
AB298505.1 (Daucus carota)
DW158660.1 (Lactuca virosa)
EH674179.1 (Cichorium intybus)
DY974866.1 (Lactuca sativa)
GdMYBML4 (Gorteria diffusa)
GE609305.1 (Cynara scolymus)
EL386329.1 (Carthamus tinctorius)
GE565436.1 (Guizotia abyssinica)
EL457760.1 (Helianthus tuberosus)
EL479041.1 (Helianthus paradoxus)
ES595589.1 (Eucalyptus globulus)
EX658114.1 (Fragaria vesca)
EX678642.1 (Fragaria vesca)
EX261861.1 (Carica papaya)
ES441147.1 (Theobroma cacao)
Medtr7g010480.1 [MtMYBML3] (Medicago truncatula)
XM002533940.1 (Ricinus communis)
XM002283807.1 (Vitis vinifera)
GO243958.1 (Olea europaea)
CO090668.1 (Gossypium raimondii)
XM002311277 [PtMYB186] (Populus trichocarpa)
cassava360.m1 (Manihot esculenta)
DV147569.1 (Euphorbia esula)
ppa006769m (Prunus persica)
EB142336.1 (Malus domestica)
FP026752.1 (Quercus robur)
DY296793.1 (Citrus clementina)
Glyma09g37040.1 (Glycine max)
Glyma13g05550.1 (Glycine max)
FS274986.1 (Glycyrrhiza uralensis)
MYBML8 (Lotus corniculatus)
MYBML64 (Coronilla scorpioides)
MYBML64 (Lotus tetragonolobus)
MYBML64 (Lotus garciniae)
MYBML64 (Robinia pseudoacacia)
MYBML64 (Vicia unijuga)
FG532960.1 (Pisum sativum)
Medtr6g013190.1 (Medicago truncatula)
EX071980.1 (Brassica rapa)
FD551900.1 (Raphanus raphanistrum)
NM121535.3 [AtMYB16] (Arabidopsis thaliana)
488379 (Arabidopsis lyrata)
477416 (Arabidopsis lyrata)
NM110979.2 [AtMYB106/NOK] (Arabidopsis thaliana)
DN773915.1 (Eutrema salsugineum)
EV567014.1 (Raphanus raphanistrum)
EX045164.1 (Brassica rapa)
Z13996.1 (Petunia hybrida)
FS417072.1 (Nicotiana tabacum)
GO605614.1 (Nicotiana benthamiana)
CA516461.1 (Capsicum annuum)
DB707584.1 (Solanum lycopersicum)
BF054497.1 (Solanum tuberosum)
ScaMYBML (Solanum capsicoides)
ScoMYBML (Solanum cortaceum)
SsMYBML (Solanum sysimbifolium)
SeMYBML (Solanum elaeagnifolium)
StMYBML (Solanum tridynamum)
MIXTA - like
0.3

FIGURE 3

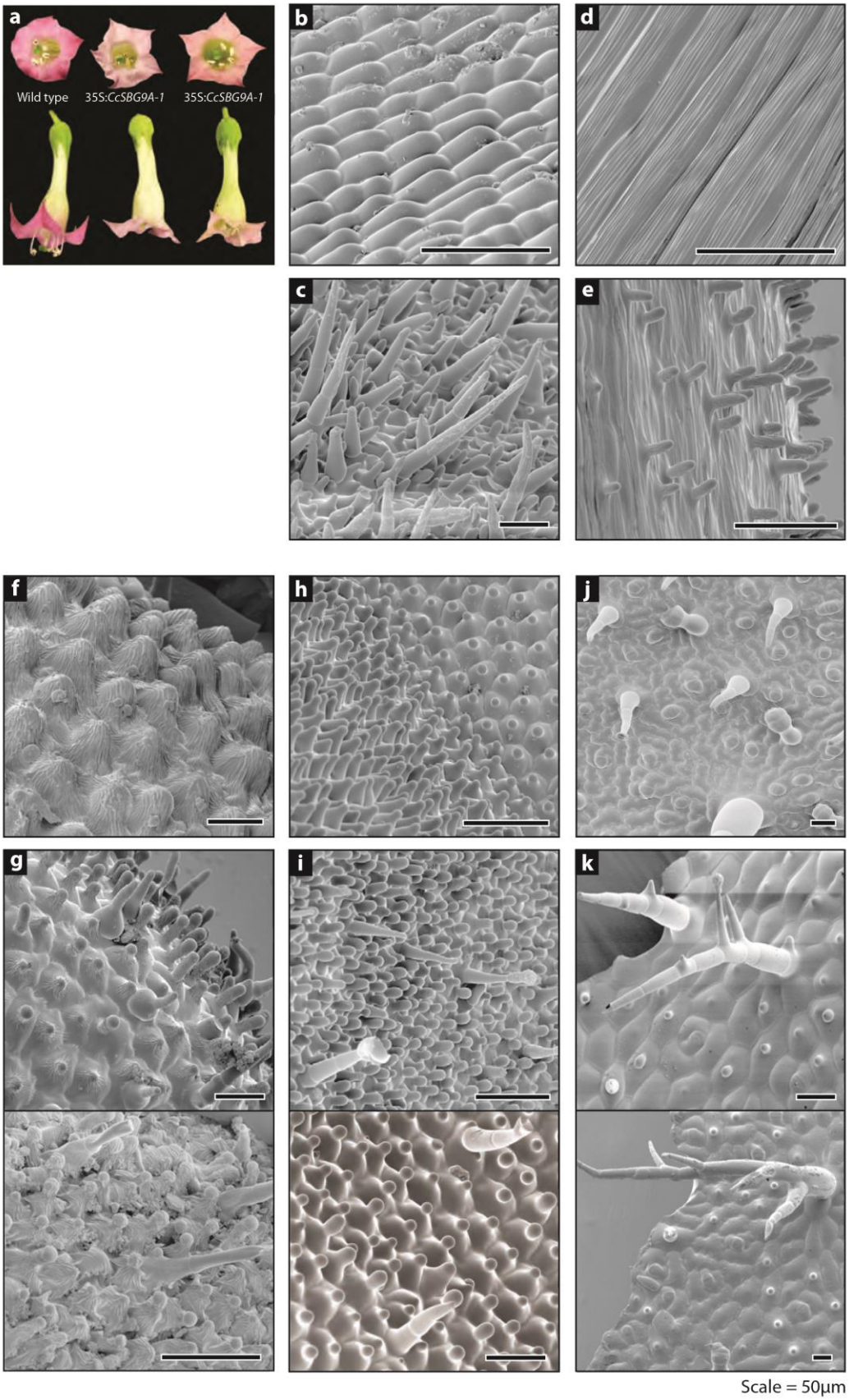
a
Wild type
35S:CcSBG9A-1
35S:CcSBG9A-1
b
d
c
e
f
h
j
g
i
k
Scale = 50µm

FIGURE 4

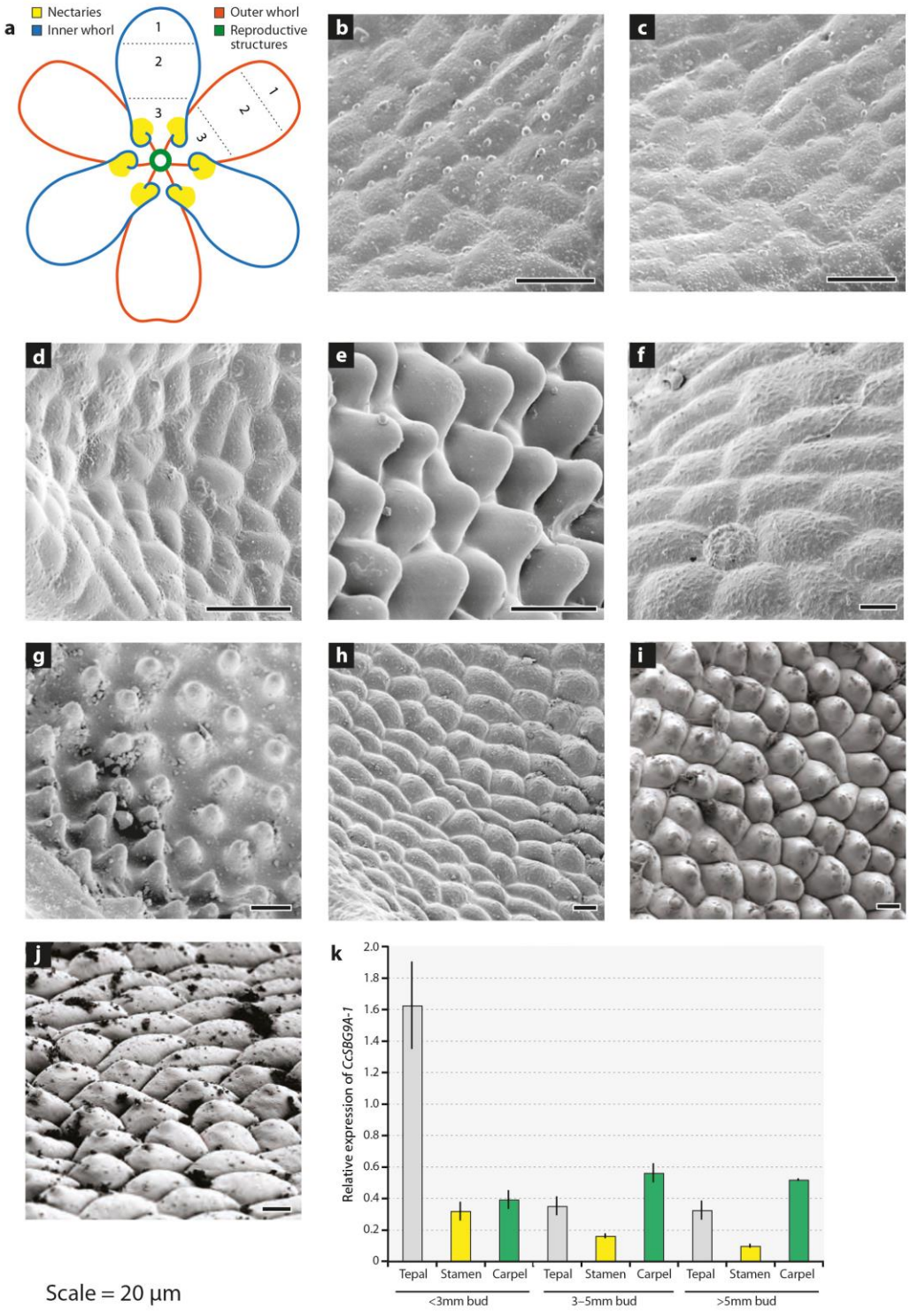
a
Nectaries
Inner whorl
Outer whorl
Reproductive structures
1
2
3
1
2
3
b
c
d
e
f
g
h
i
j
k
Relative expression of CcSBG9A-1
2.0
1.8
1.6
1.4
1.2
1.0
0.8
0.6
0.4
0.2
0
Tepal
Stamen
Carpel
Tepal
Stamen
Carpel
Tepal
Stamen
Carpel
<3mm bud
3–5mm bud
>5mm bud
Scale = 20 µm

FIGURE 5